

Third-order optical nonlinearity of C₆₀, C₇₀, and CS₂ in benzene at 1.06 μm

N. Tang, J. P. Partanen, R. W. Hellwarth, and R. J. Knize

University of Southern California, Departments of Electrical Engineering and Physics, Los Angeles, California 90089-0484

(Received 10 February 1993)

By measuring the third-order nonlinear optical susceptibility $\chi_{1111}^{(3)}(-\omega, \omega, \omega, -\omega)$ at 1.06 μm of various solutions of C₆₀ and C₇₀ in benzene, we place limits on the hyperpolarizabilities of these molecules of $-180 \leq (\gamma_{1111}^{C_{60}}/\gamma_{1111}^{\text{benzene}}) \leq 60$ and $-120 \leq (\gamma_{1111}^{C_{70}}/\gamma_{1111}^{\text{benzene}}) \leq 250$, respectively. These limits assume that 1.06 μm is near the long-wavelength limit where $\chi^{(3)}$ must be real. We also give limits on the imaginary parts of the hyperpolarizabilities, making no assumptions about their phases. The magnitudes of these limits are two orders of magnitude smaller than several values that have been published. We checked our experimental technique by measuring the nonlinear susceptibility of CS₂-benzene mixtures and found the value for $\chi_{CS_2}^{(3)}/\chi_{\text{benzene}}^{(3)}$ of 5.7 ± 0.5 . This agrees with parameters deduced from many different experiments published previously.

Fullerenes possess highly delocalized electrons and so are expected to exhibit optical behavior similar to linear conjugated polymers.¹ That is, fullerenes are expected to exhibit larger (nonresonant) linear and nonlinear optical polarizabilities per carbon atom than, for example, benzene. The nonlinear molecular characteristic most accessible to theory is the "hyperpolarizability," commonly called γ_{1111} . This, along with the linear polarizability α , relates the amplitude M_x of the x component $m_x(t)$ of the electric dipole moment of a molecule to the amplitude E_x of the x component of the optical field at ω . With $m_x(t) = \text{Re}(M_x e^{-i\omega t})$, and similarly for E_x , one may write this relation as

$$M_x = \alpha E_x + 3\gamma_{1111} E_x |E_x|^2. \quad (1)$$

The value of γ_{1111} for linear conjugated polymers in the low-frequency limit (well below any absorption bands) has been predicted to increase with chain length approximately as a power law with a power near 4.² The predictions are in reasonable agreement with experiments.^{2,3}

The highest solubility of C₆₀ and C₇₀ without chemical change appears to occur in toluene, and these molecules are only slightly less soluble in benzene. Therefore such solutions are an obvious choice for optical measurements on C₆₀ in its ground electronic state. The first nonlinear optics measurements on C₆₀ in such solutions were of degenerate four-wave mixing (DFWM) at 1.06 μm, a wavelength long enough that results should be near the long-wavelength limit.^{1,4,5} Two of these measurements gave hyperpolarizability values for C₆₀ that were more than three orders of magnitude larger *per carbon* than for benzene. The hyperpolarizability for C₇₀ was measured to be four orders of magnitude larger *per carbon* than for benzene.⁶ However, the measurements quoted in Refs. 4 and 6 were done with lasers having pulse lengths longer than 5 ns. In the nanosecond time scale, thermal effects play important roles even in transparent media.⁷ Therefore such long pulses are unsuitable for this kind of measurement. The two remaining solution measurements^{1,5} with picosecond pulses disagree by many orders of magnitude

even after the three-orders-of-magnitude correction^{5,8} in the value of Ref. 1. The value attributed to Ref. 1 in the review article Ref. 9 also differs from the experimental data shown in Ref. 1 by more than an order of magnitude. One aim of this paper is to narrow this range of uncertainty.

In this paper we measure γ_{1111} of C₆₀ in solution at 1.06 μm by degenerate four-wave mixing and find an upper bound on the hyperpolarizabilities that is not significantly larger *per carbon* than for benzene (if γ_{1111} is real, as is expected in the low-frequency limit). We also obtain an upper bound for the imaginary part of γ_{1111} which must exist as the optical frequency ω approaches an electronic resonance in the molecule. We repeat the measurements with C₇₀ and find again an upper limit for the magnitude of the hyperpolarizability that is orders of magnitude smaller than previously reported.⁶ We check that our results, although contradicting some of the literature,^{1,4,6} are valid, as follows. We use the same apparatus and procedure to measure the hyperpolarizability of CS₂ dissolved in benzene versus concentration. Our results are consistent with literature values and give, to our knowledge, the most accurate measurement of the hyperpolarizability ratio between CS₂ and benzene. Our limits on the hyperpolarizability of C₆₀ obtained from the C₆₀-benzene solutions are consistent with a null result reported without limits for the similar solutions by Kafafi *et al.*⁵

We prepare the fullerenes, C₆₀ and C₇₀, by the carbon-arc evaporation method.¹⁰ Column chromatography is used to separate and purify the samples.^{11,12} Magenta solutions of C₆₀-benzene and dark brown solutions of C₇₀-benzene with concentrations up to 2.5 and 2.0 g/l, respectively, are obtained. Visible and infrared (IR) absorption spectra of these solutions are compared to the known spectra to establish that the purity of the solute is greater than 95%.¹²

In our experiment, a standard DFWM setup is employed as shown in Fig. 1. A mode-locked Nd:YAG (where YAG denotes yttrium aluminum garnet) laser

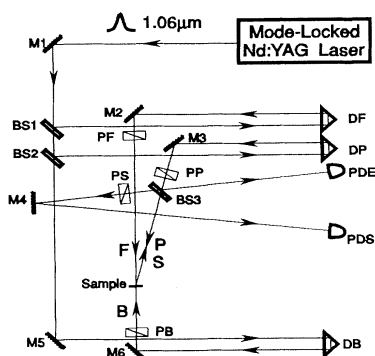


FIG. 1. Experimental arrangement. Polarizations of forward (F), backward (B), probe (P), and signal (S) beams are controlled by polarizers PF , PB , PP , and PS . The crossing angle between F and P is about 17° . $M1$ to $M6$ are six mirrors, $BS1$ to $BS3$ are three beam splitters, DF , DP , and DB are delay lines, and PDE and PDS are photodiodes.

pulse of ~ 30 psec at $1.06 \mu\text{m}$ is split into the three beams: F , B , and P of energies ~ 1 , 1 , and 0.2 mJ, respectively. Each beam has a diameter ~ 3 mm in the sample. The F and B beams are aligned to counterpropagate while beam P crosses beam F at an angle of 17° . The signal beam S generated by the nonlinear interaction propagates counter to beam P . Sample solutions are contained in a 1-mm-thick spectrophotometer cell. The pulses in the three beams F , B , and P are adjusted to overlap at the sample. Then either the F , B , or P pulse is delayed as shown in Fig. 1. The polarizations of all four beams are controlled by the polarizers PF , PB , PP , and PS in Fig. 1 to allow measurements of different tensor components of the third-order nonlinear optical susceptibility $\chi^{(3)}$. Input and signal pulse energies are measured by photodiodes and fed into the A/D converter port of a PC.

The DFWM signal for various C_{60} and C_{70} concentrations in benzene, with three parallel-polarized temporally overlapping pulses, is shown in Figs. 2(a) and 3(a), respectively. We find that the signal is proportional to the product of the three input energies up to at least five times higher than the energies used in our experiments. For each laser pulse, a normalized signal energy U_s is obtained by dividing the signal by the product of the three input energies. To reduce shot-to-shot variation, we average 100 shots in each trial. Small differences in the position of the sample can cause a 10% variation in the signal. The error from this variation is reduced by taking T (~ 5) trials with the unknown sample alternately with T trials with a pure benzene reference. The error bar given with each data point is calculated as follows. We form $2T-1$ ratios between adjacent (sample/reference) trials. The standard deviation of these numbers is divided by $\sqrt{2T-1}$ and expressed as half the error bar shown. By this method, we obtain a measurement of the sample relative to the reference that is repeatable to within a few percent.

To verify that the DFWM signal was essentially instantaneous on the picosecond time scale involved, we remeasured all of these points as a function of the delay time of

the backward delay beam B . All samples exhibited essentially instantaneous time behavior such as shown in Fig. 4 for a pure benzene sample without any further features up to several nanoseconds.

To check our measurement technique, we also measured a normalized DFWM signal energy U_s as a function of CS_2 volume fraction v in a CS_2 -benzene mixture, and did observe the variation shown in Fig. 5, which is in agreement with the theory given below. The height of the data point box in Fig. 5(a) represents the vertical error bar following the same procedure as in the cases of C_{60} and C_{70} , while the width of the box accounts for the uncertainty in CS_2 concentration.

When the nonlinearity can be considered instantaneous, the energy U_s of the weak signal beam can be expressed as¹³

$$U_s = K \frac{I_e^2}{n^4} |\chi_{1111}^{(3)}|^2, \quad (2)$$

where $\chi_{1111}^{(3)}$ has the definition of the $c_{1111}^{(3)}(-\omega, \omega, \omega, -\omega)$

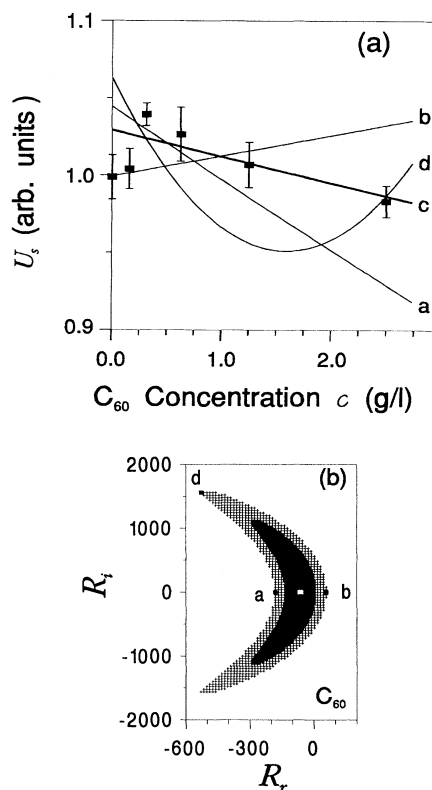


FIG. 2. (a) Concentration dependence of the normalized degenerate-four-wave-mixing signal energy U_s of C_{60} -benzene solutions. The thicker line c corresponds to the absolute χ^2 minimum. Lines a , b , and d are plots of Eq. (6) with the parameters of the points labeled a , b , and d in (b), respectively. (b) The dark shaded region contains all parameter pairs (R_r, R_i) which, in comparing Eq. (6) with the data, give χ^2 values less than twice the minimum, which occurs at the "best-fit" values indicated by the center blank. The boundary of the lighter shaded region contains parameter pairs whose χ^2 values are less than four times the minimum.

coefficient defined by Maker and Terhune¹⁴ and by Hellwarth.¹⁵ Here n is the refractive index, l_e is the effective interaction length, and K is a constant which contains all the factors (geometry, laser characteristics, etc.) that remain the same from sample to sample, and which has been discussed elsewhere.¹³ Because we observe no effect of absorption at any points in Figs. 2–5, we take l_e to be simply the sample thickness (1 mm).

In the standard (but approximate) theory, $\chi_{1111}^{(3)}$ is related to the molecular hyperpolarizability γ_{1111} of the two composites by

$$\chi_{1111}^{(3)} = (N_1\gamma_{1111}^1 + N_2\gamma_{1111}^2)L^4, \quad (3)$$

where N_i are the number densities, γ_{1111}^i the molecular hyperpolarizabilities for the two components ($i=1,2$), and L is a local-field factor which is related to the linear refractive index n of the mixture by $L = (n^2 + 2)/3$. We use the Lorentz-Lorenz relation to calculate n , a step which we believe introduces negligible error:

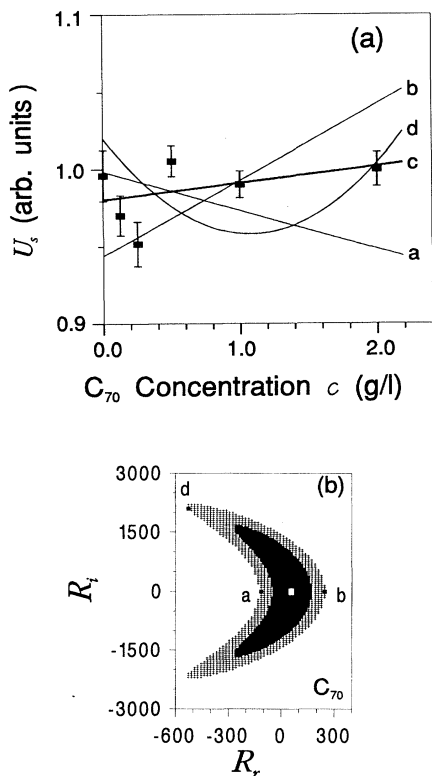


FIG. 3. (a) Concentration dependence of the normalized degenerate-four-wave-mixing signal energy U_s of C_{70} -benzene solutions. The thicker line c corresponds to the absolute χ^2 minimum. Lines a , b , and d are plots of Eq. (6) with the parameters of the points labeled a , b , and d in (b), respectively. (b) The dark shaded region contains all parameter pairs (R_r, R_i) which, in comparing Eq. (6) with the data, give χ^2 value less than twice the minimum, which occurs at the “best-fit” values indicated by the center blank. The boundary of the lighter shaded region contains parameter pairs whose χ^2 values are less than four times the minimum.

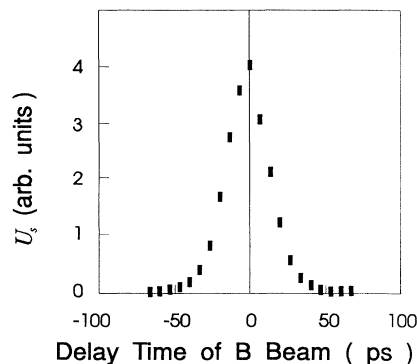


FIG. 4. Temporal response of the DFWM signal for a pure benzene sample. All samples under investigation in this paper show indistinguishable behavior. Longer delay time up to a few nanoseconds reveals no other features.

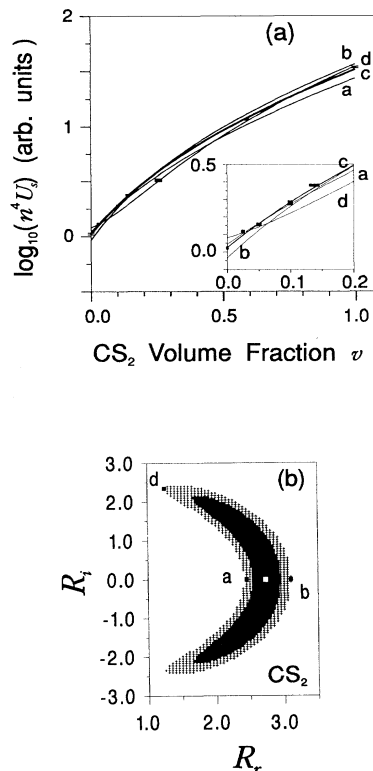


FIG. 5. (a) The logarithm of the normalized degenerate-four-wave-mixing signal energy U_s times the fourth power of the refractive index n of CS_2 -benzene mixtures measured at various volume fractions v of CS_2 in benzene. The thicker line c corresponds to the absolute χ^2 minimum obtained from fitting the data to Eq. (7). Lines a , b , and d are plots of Eq. (7) with the parameters of the points labeled a , b , and d in (b), respectively. (b) The dark shaded region contains all parameter pairs (R_r, R_i) which, in comparing Eq. (7) with the data, give χ^2 values less than twice the minimum, which occurs at the “best-fit” values indicated by the center blank. The boundary of the lighter shaded region contains parameter pairs whose χ^2 values are less than four times the minimum.

$$\frac{n^2-1}{n^2+2} = \frac{4\pi}{3} \sum_{i=1,2} N_i \alpha_i. \quad (4)$$

Here the α_i are the linear polarizabilities of the two components. Cubic crystals of C₆₀ have refractive index $n=2.0$ and density 8.3×10^{22} carbon atoms/cm³, giving polarizability $\alpha=1.4 \times 10^{-24}$ cm³ per carbon atom. This formula gives similarly $\alpha=1.6 \times 10^{-24}$ cm³ for each C-H unit in liquid benzene. If electron delocalization is reflected in linear polarizability,¹ then the measured values of linear polarizability suggest very little electron delocalization.

In the C₆₀ and C₇₀ solutions, the refractive index change from the pure benzene is negligible due to the small C₆₀ and C₇₀ concentration. In the CS₂-benzene case, from the data in Ref. 16, we see that the total volume of our CS₂-benzene solutions changes less than 1% upon mixing. Neglecting this change, we rewrite (4) as

$$\frac{n^2-1}{n^2+2} = \frac{n_{\text{CS}_2}^2-1}{n_{\text{CS}_2}^2+2} \nu + \frac{n_{\text{benzene}}^2-1}{n_{\text{benzene}}^2+2} (1-\nu), \quad (5)$$

where n_{CS_2} and n_{benzene} are the refractive indices of CS₂ and benzene, and the ν is the volume fraction of CS₂ in the mixture.

From our data we determine the range of the complex hyperpolarizabilities of the C₆₀ and C₇₀ molecules relative to benzene, which is consistent with our data assuming that the hyperpolarizability of benzene is real and positive. The method involves calculating “ χ^2 ” functions using the experimental points and the following theoretical expression for the normalized signal energy U_s derived from (2)–(5) with the assumptions that the refractive index n and the density of benzene molecules are constant.

$$U_s = K' [1 + 2AR_r c + A^2(R_r^2 + R_i^2)c^2]. \quad (6)$$

The molecular concentration c is in grams per liter (g/l). From the parameters in Table I, we evaluate $A=1.2067 \times 10^{-4}$ l/g for C₆₀ and $A=1.0343 \times 10^{-4}$ l/g for C₇₀. We vary the parameters K' , R_r , and R_i , first to

$$n^4 U_s = K'' \frac{1 + 2(AR_r - 1)\nu + [1 + A^2(R_r^2 + R_i^2) - 2AR_r]\nu^2}{(1 - B\nu)^8}. \quad (7)$$

Here $A=1.4742$ and $B=0.07710$ are two constants calculated from the data in Table I, and K'' is a factor which is the same for transparent samples of the same length in identical beams. Fitting our data to this relation, we obtain the regions in the (R_r, R_i) plane shown in Fig. 5(b) that have χ^2 values less than twice (dark) and four times (light) the “best-fit” χ^2 minimum. This minimum is indicated by the blank box in the center of Fig. 5(b). The standard theory for uncorrelated and normally distributed errors would label the lighter and the darker regions with a probability of 0.999 and 0.9, respectively.¹⁸ Since R_i is expected from theory to be negligible

TABLE I. Parameters used in converting data to hyperpolarizability values. Temperature is assumed to be 20°C. Digits in parentheses give estimated uncertainty in last digit.

Liquid	Density (g/cm ³) ^a	Refractive index at 1.06 μm ^b	Molecular mass (g/mol) ^a
Benzene	0.879	1.4825(5)	78.11
CS ₂	1.263	1.5964(5)	76.13

^aReference 17.

^bFrom Sellmeier formulas of Ref. 15.

find those which make χ^2 minimum, and then to find the ranges in which χ^2 is below twice or four times this minimum. Physically, the parameter K' is determined by beam geometry in a manner discussed in Ref. 13. R_r and R_i are the real and imaginary parts of the carbon molecule hyperpolarizability normalized to the real positive hyperpolarizability of a benzene molecule. In Figs. 2(b) and 3(b) we show the regions in (R_r, R_i) parameter space in which the χ^2 function of the data referred to the relation (6) is less than twice (darker region) and four times (lighter region) the absolute χ^2 minimum at which we obtain the “best-fit” values indicated by the blank box in the center.^{18,19} If the experimental errors were uncorrelated and normally distributed (which is unlikely), the true (R_r, R_i) values would have a probability of 0.99 to lie within the bounds of the lighter shaded area, and a probability of 0.7 to lie within the darker shaded area, according to the standard theory.¹⁸

At our experimental wavelength of 1.06 μm , all our samples showed unmeasurable absorption; the first electronic excitations are at much higher frequencies. In these circumstances, there is no known theoretical or experimental example in which $\gamma_{1111}(-\omega, \omega, \omega, -\omega)$ is not nearly a real positive number. In interpreting our data we will assume that this is the case in all our samples, while continuing to give the unrestricted ratios R_r and R_i that are consistent with our present experiments.

In the case of CS₂, the change of refractive index n is taken into account with (5), our Eqs. (1)–(4) lead to the relation for the normalized signal energy U_s ,

at 1.06 μm , we find $R_r=2.7 \pm 0.3$, which gives $\chi_{\text{CS}_2}^{(3)}/\chi_{\text{benzene}}^{(3)}=5.7 \pm 0.5$ [see (3)]. The error margins are defined from the boundary of the lighter shaded area in Fig. 5(b).

We summarize what the experimental literature suggests for the values of $\chi_{1111}^{(3)}(-\omega, \omega, \omega, -\omega)$ for CS₂ and benzene as follows. We use the (approximate) dispersion formulas (13.1) and (13.3) for $\chi^{(3)}$ in Ref. 15 with the long-wavelength parameters for CS₂ and benzene proposed there in Secs. 14.4 and 14.5. These parameters were derived from dozens of reported measurements of seven different nonlinear effects (see Figs. 13.1 and 13.2)

made at a wide variety of wavelengths and collated with the aforementioned dispersion formulas. The resulting $\chi_{1111}^{(3)}$ value for CS₂ is $(47 \pm 5) \times 10^{-14}$ esu, and for benzene it is $(8.3 \pm 1.4) \times 10^{-14}$ esu at 1.06- μm wavelength. This agrees with the more accurate result quoted above and pictured in Fig. 5. To convert our results for C₆₀ and C₇₀, which are relative to benzene, to absolute values, we recommend using the value of $\chi_{1111}^{(3)}(-\omega, \omega, \omega, -\omega) = (8 \pm 1) \times 10^{-14}$ esu for benzene at 1.06 μm , and the formulas (13.1) and (13.3) of Ref. 15 to estimate the dispersion.

Kafafi *et al.*,²⁰ have measured the $\chi^{(3)}$ at 1.06 μm of a 21- μm film of C₆₀ on a BaF₂ substrate and found it to be 7×10^{-12} esu, if the value for CS₂ is 0.4×10^{-12} esu. They did not discuss the uncertainty of the comparison or of their data. If one takes the ratio of their preferred line in their Fig. 2 to be exactly (70/4), then the spread in data in that figure would suggest that this ratio is somewhere between 12 and 25. Then if one uses our Eq. (3) with the above $\chi_{1111}^{(3)}$ for CS₂ to calculate γ_{1111} for C₆₀, one obtains values in the range 60–200 times the value of γ_{1111} of benzene. Assuming, as we have explained, that this $\chi_{1111}^{(3)}$ is real and positive, this is just consistent with our upper limit of 60. We believe this makes 60 a much more likely value than 200.

In conclusion, we have measured the third-order nonlinear optical susceptibility $\chi_{1111}^{(3)}(-\omega, \omega, \omega, -\omega)$ of various solutions of C₆₀ and C₇₀ at 1.06 μm , and were able to place limits surrounding zero on the hyperpolarizabilities

of these molecules. If we take the conservative limits which include χ^2 values up to four times the absolute minimum of the χ^2 function, we find ranges $-180 \leq [\gamma_{1111}^{C_{60}} / \gamma_{1111}^{\text{benzene}}] \leq 60$ for C₆₀, and $-120 \leq [\gamma_{1111}^{C_{70}} / \gamma_{1111}^{\text{benzene}}] \leq 250$ for C₇₀ respectively, to be consistent with our data. This assumes that 1.06 μm is near the long-wavelength limit where the $\chi^{(3)}$ must be real (and, we believe, also positive). We also give limits on the imaginary parts of the hyperpolarizabilities, making no assumptions about their phases. Our data suggest that, if electron delocalization causes the hyperpolarizability per carbon unit to increase with the number of units, then the electrons in the ground states of C₆₀ and C₇₀ are not significantly more delocalized than the electrons in benzene. This conclusion is consistent with the fact that the linear polarizability per carbon unit is not larger for C₆₀ than for benzene. However, these ideas await definite theory. We checked our experimental technique by measuring the nonlinear susceptibility of CS₂-benzene mixtures and find the dependence expected from the same standard theory used to analyze the fullerenes. The new, more accurate value for $\chi_{CS_2}^{(3)} / \chi_{\text{benzene}}^{(3)}$ of 5.7 ± 0.5 is obtained at 1.06 μm .

This research was supported by the U.S. Air Force Office of Scientific Research under Grant No. F49620-91-C-0018. The authors would like to thank Dr. M. McLean for help in preparing the C₆₀ and C₇₀ samples.

- ¹W. J. Blau, H. J. Byrne, D. J. Cardin, T. J. Dennis, J. P. Hare, H. W. Kroto, R. Taylor, and D. R. M. Walton, *Phys. Rev. Lett.* **67**, 1423 (1991).
- ²S. Mukamel and H. X. Wang, *Phys. Rev. Lett.* **69**, 65 (1992); J. R. Heflin, K. Y. Wong, O. Zamani-Khamiri, and A. F. Garito, *Phys. Rev. B* **38**, 1573 (1988); K.C. Rustagi and J. Ducuing, *Opt. Commun.* **10**, 258 (1974).
- ³J. P. Hermann and J. Ducuing, *J. Appl. Phys.* **45**, 5100 (1974).
- ⁴Q. Gong, Y. Sun, Z. Xia, Y. H. Zou, Z. Gu, X. Zhou, and D. Qiang, *J. Appl. Phys.* **71**, 3025 (1992).
- ⁵Z. H. Kafafi, F. J. Bartoli, J. R. Lindle, and R. G. S. Pong, *Phys. Rev. Lett.* **68**, 2705 (1992).
- ⁶S. Yang, Q. Gong, Z. Xia, Y. H. Zhou, Y. Q. Wu, D. Qiang, Y. L. Sun, and Z. N. Gu, *Appl. Phys. B* **55**, 51 (1992).
- ⁷G. Martin and R. W. Hellwarth, *Appl. Phys. Lett.* **34**, 371 (1979).
- ⁸R. J. Knize and J. P. Partanen, *Phys. Rev. Lett.* **68**, 2704 (1992).
- ⁹W. J. Blau and D. J. Cardin, *Mod. Phys. Lett. B* **6**, 1351 (1992).
- ¹⁰W. Kratschmer, L. D. Lamb, K. Fostiropoulos, and D. R. Huffman, *Nature* **V347**, 354 (1990).
- ¹¹R. Taylor, J. P. Hare, A. K. Abdul-Sada, and H. W. Kroto, *Chem. Commun.* **1990**, 1423.
- ¹²H. Ajie, M. M. Alvarez, S. J. Anz, R. D. Beck, F. Diederich, K. Fostiropoulos, D. R. Huffman, W. Kratschmer, Y. Rubin, K. E. Schriver, D. Sensharma, and R. L. Whetten, *J. Phys. Chem.* **94**, 8630 (1990).
- ¹³X. F. Cao, J. P. Jiang, D. P. Bloch, R. W. Hellwarth, L. P. Yu, and L. Dalton, *J. Appl. Phys.* **65**, 5012 (1989).
- ¹⁴P. D. Maker and R. W. Terhune, *Phys. Rev.* **137**, A801 (1965).
- ¹⁵R. W. Hellwarth, *Prog. Quantum. Electron.* **5**, 1 (1977).
- ¹⁶*International Critical Tables of Numerical Data, Physics, Chemistry and Technology* (McGraw-Hill, New York, 1928), Vol. III.
- ¹⁷*American Institute of Physics Handbook* (McGraw-Hill, New York, 1963).
- ¹⁸W. H. Press, B. P. Flannery, S. A. Teukosky, and W. T. Vetterling, *Numerical Recipes in Pascal* (Cambridge University Press, Cambridge, 1989), Chap. 14.
- ¹⁹P. R. Bevington, *Data Reduction and Error Analysis for the Physical Sciences* (McGraw-Hill, New York, 1969).
- ²⁰Z. H. Kafafi, J. R. Lindle, R. G. S. Pong, F. J. Bartoli, L. J. Lingg, and J. Milliken, *Chem. Phys. Lett.* **188**, 492 (1992).